Knockdown of exosome-mediated lnc-PVT1 alleviates lipopolysaccharide-induced osteoarthritis progression by mediating the HMGB1/TLR4/NF-κB pathway via miR-93-5p

YONG MENG[1,2], SIQIANG QIU[3], LONG SUN[2] and JINLIANG ZUO[3]

[1]Qingdao University, Qingdao, Shandong 266000; [2]Department of Orthopedics, Weihai Municipal Hospital, Weihai, Shandong 264200; [3]Department of Spine Surgery, The Fourth People's Hospital of Jinan, Jinan, Shandong 250031, P.R. China

Received December 13, 2019; Accepted September 2, 2020

DOI: 10.3892/mmr.2020.11594

Abstract. Osteoarthritis is a chronic degenerative joint disease. Long non-coding RNA plasmacytoma variant translocation 1 (PVT1) is involved in the progression of osteoarthritis and exosomes serve a central role in intercellular communication. However, whether PVT1 can be mediated by exosomes in osteoarthritis has not been reported. Whole blood was drawn from osteoarthritis patients and healthy volunteers. Lipopolysaccharide (LPS) was used to stimulate human normal chondrocytes (C28/I2) to construct a cell damage model *in vitro*. Protein levels were examined via western blot analysis. eThe expression of PVT1, microRNA (miR)-93-5p and high mobility groupprotein B1 (HMGB1) was evaluated through reverse transcription-quantitative PCR. Cell viability and apoptosis were determined through CCK-8 or flow cytometric assay. Inflammatory cytokines were measured via ELISA. The relationship between PVT1 or HMGB1 and miR-93-5p was confirmed by dual-luciferase reporter assay. PVT1, HMGB1 and exosomal PVT1 were upregulated while miR-93-5p was downregulated in osteoarthritis patient serum and LPS-induced C28/I2 cells. Exosomes from osteoarthritis patient serum and LPS-treated C28/I2 cells increased PVT1 expression in C28/I2 cells. PVT1 depletion reversed the decrease of viability and the increase of apoptosis, inflammation responses and collagen degradation of C28/I2 cells induced by LPS. PVT1 regulated HMGB1 expression via sponging miR-93-5p. miR-93-5p inhibition abolished PVT1 silencing-mediated viability, apoptosis, inflammation responses and collagen degradation of LPS-stimulated C28/I2 cells. HMGB1 increase overturned miR-93-5p upregulation-mediated viability, apoptosis, inflammation responses and collagen degradation of LPS-stimulated C28/I2 cells. Furthermore, PVT1 modulated the Toll-like receptor 4/NF-κB pathway through an miR-93-5p/HMGB1 axis. In summary, exosome-mediated PVT1 regulated LPS-induced osteoarthritis progression by modulating the HMGB1/TLR4/NF-κB pathway via miR-93-5p, providing a new route for possible osteoarthritis treatment.

Correspondence to: Dr Jinliang Zuo, Department of Spine Surgery, The Fourth People's Hospital of Jinan, 50 Shifan Road, Tianqiao, Jinan, Shandong 250031, P.R. China
E-mail: alecmed@163.com

Key words: osteoarthritis, exosomes, plasmacytoma variant translocation 1, miR-93-5p, high mobility group protein B1, Toll-like receptor 4/NF-κB

Introduction

Osteoarthritis is a common chronic degenerative joint disease characterized by synovial inflammation and cartilage protein degradation (1). Osteoarthritis can cause pain and disability, and it will become the largest disability problem in the United States by 2030 (2). Unfortunately, there are no effective treatments that can change the progression of osteoarthritis (3). Currently, osteoarthritis is mainly treated with a regimen that controls symptoms and relieves pain (4). Therefore, it is essential to explore the pathogenesis of osteoarthritis for the development of effective osteoarthritis treatment programs.

Long non-coding RNAs (lncRNAs) are a type of non-protein-encoding RNAs >200 nucleotides in length, which exert crucial regulatory roles in gene regulatory networks (5). lncRNAs are implicated in vital physiological processes, such as cell lineage determination, cell differentiation, organogenesis and tissue homeostasis (6). Previous studies have demonstrated that lncRNAs are involved in the progression of osteoarthritis (7-9). For example, lncRNA FOXD2-AS1 was revealed to modulate the proliferation of chondrocytes in osteoarthritis (9). lncRNA plasmacytoma variant translocation 1 (PVT1), also known as LINC00079, MIR1204HG, or onco-lncRNA-100, is associated with the progression of a range of tumors (10). PVT1 has been revealed to accelerate lipopolysaccharide (LPS)-induced septic acute kidney injury (11). PVT1 was demonstrated to impede cardiac function and facilitate the secretion of inflammatory factors in a sepsis model (12). Additionally, PVT1 has been revealed to modulate the apoptosis of chondrocytes in osteoarthritis (13). Nevertheless, the role of PVT1 and its

molecular mechanisms in the pathogenesis of osteoarthritis remain to be elucidated.

MicroRNAs (miRNAs) are another crucial class of non-coding RNAs that bind to complementary mRNAs, resulting in translation inhibition or degradation of mRNA (14). miRNAs serve vital roles in cell differentiation and metabolism, organ development, viral infection and tumorigenesis (15). miRNA-93-5p (miR-93-5p) serves different functions in different tumors (16,17). In addition, miR-93-5p can suppress osteogenic differentiation (18). miR-93-5p has also been implicated in the inflammatory and antiproliferative processes of human bronchial epithelial cell lines induced by neodymium oxide (19). Furthermore, miR-93-5p has been revealed to regulate IL-1β-induced cartilage degradation and chondrocyte apoptosis in osteoarthritis (20). However, the role of miR-93-5p in osteoarthritis remains to be elucidated.

Exosomes are small extracellular vesicles with a lipid bilayer member structure that can be secreted by most cells and have a diameter of ~30-100 nm (21). Exosomes contain cell-specific proteins, lipids and nucleic acids that can be transmitted as signal molecules to other cells to alter their function (22,23). Small extracellular vesicles may exert a role in the pathogenesis of a variety of inflammatory diseases (24). For instance, HIF-1α-induced exosomal miR-23a can activate macrophages and promote tubulointerstitial inflammation (25). In addition, the exosomal MALAT1 derived from adipose-derived stem cells regulates inflammation-related networks and promotes regeneration after traumatic brain injury (26). A previous study reported that exosomes released from synovial fibroblasts in patients with rheumatoid arthritis contain TNF-α membrane forms, which could make activated T cells resistant to apoptosis and contribute to the pathogenic process of rheumatoid arthritis (27). However, the function of exosomal PVT1 in the development of osteoarthritis is unclear.

Hence, the present study explored the expression of exosomal PVT1 in the serum of patients with osteoarthritis and in an osteoarthritis cell model (LPS-stimulated C28/I2 cells) *in vitro*. The effect of exosomes of LPS-stimulated C28/I2 cells and the serum of patients with osteoarthritis on the expression of exosomal PVT1 in C28/I2 cells was investigated. The present study also explored the role of PVT1 in the viability, apoptosis and inflammation responses of LPS-stimulated C28/I2 cells and its molecular mechanisms to provide possible therapeutic tactics for the treatment of osteoarthritis.

Materials and methods

Osteoarthritis subjects. The present study was authorized by the Ethics Committee of Weihai Municipal Hospital. A total of 30 osteoarthritis patients (19 females and 1 males, age range from 50 to 70 years old) and 30 healthy volunteers (19 females and 11 males, age range from 50 to 70 years old) were recruited from Weihai Municipal Hospital between October 2017 and June 2019. Whole blood (20 ml) was drawn from each osteoarthritis patient and healthy volunteer. The blood sample was kept at room temperature for 2 h and centrifuged (4˚C, 1,200 x g, 20 min) to acquire serum. Serum was stored in liquid nitrogen for subsequent studies. All patients with osteoarthritis and the healthy subjects who participated in the present study signed written informed consent.

Cell culture and treatment. Human normal chondrocytes C28/I2 were acquired from BeNa Culture Collection. Dulbecco's modified Eagle's medium/F-12 medium (1:1, DMEM/F-12; HyClone; Cytiva) containing fetal bovine serum (10%, FBS, HyClone; Cytiva) was employed to maintain the C28/I2 cells. A humidified incubator with 5% CO_2 at 37˚C was used to maintain the C28/I2 cells. C28/I2 cells were exposed to different concentrations of LPS (1, 5 and 10 μg/ml; Sigma-Aldrich; Merck KGaA) for 48 h to construct an osteoarthritis state cell model.

Exosome isolation. Exosome-free medium (Sigma-Aldrich; Merck KGaA) was used to culture C28/I2 cells or LPS-stimulated C28/I2 cells at 37˚C for 48 h. The culture medium was collected and centrifuged (1,500 x g, 15 min) at 4˚C and the supernatant filtered through a 0.22-μm polyvinylidene difluoride (PVDF) filter (EMD Millipore). ExoQuick™ Exosome Precipitation Solution (System Biosciences, LLC) was added to the serum or filter medium and mixed. Following refrigeration for 24 h at 4˚C, the mixture was centrifuged (1,500 x g, 30 min) at 4˚C to remove the supernatant. The exosome pellets were suspended in the exosome-free medium and the ExoELISA Exosome Quantification Assay kit (System Biosciences, LLC) was used to quantify the concentration of exosomes. Western blot analysis was performed to examine the exosomal markers CD9 and CD63. C28/I2 cells were treated with 5 μg/ml exosomes.

Transmission electron microscopy (TEM). The exosome pellets were suspended in PBS and then fixed in paraformaldehyde (4%) and glutaraldehyde (4%) in PBS (0.1 M, pH 7.4) at 4˚C for 5 min. After adding a drop of the exosomal sample, the carbon-coated copper grid was immersed in a phosphotungstic acid solution (2%, pH 7.0) for 30 sec. A transmission electron microscope (JEM-1200EX; JEOL, Ltd.) at magnification, x100,000 was used to observe and assess the morphology and size of the exosomes.

Cell transfection. Small interfering RNA (siRNA) targeting PVT1 (si-PVT1) and negative control (si-NC) were procured from Shanghai GenePharma Co., Ltd., as were miRNA mimics and inhibitors targeting miR-93-5p (miR-93-5p and anti-miR-93-5p) and their negative control (miR-NC and anti-miR-NC). The sequence of high mobility grouppro-tein B1 (HMGB1; accession: NM_001363661) was cloned into the pcDNA3.1 vector (pcDNA; Invitrogen; Thermo Fisher Scientific, Inc.) to construct the overexpression vector of HMGB1 (HMGB1). Oligonucleotides (si-PVT1 (40 nM), si-NC (40 nM), miR-93-5p (50 nM), miR-NC (50 nM), anti-miR-93-5p (50 nM), anti-miR-NC (50 nM)) or plasmids were transiently transfected into C28/I2 cells using Lipofectamine® 3000 reagent (Invitrogen; Thermo Fisher Scientific, Inc.) and then cultured in DMEM/F-12 containing 5 μg/ml LPS for 48 h. The sequences were: si-PVT1 (5'-GGGUACUGGAAGUAGAAUAUU-3') and si-NC (5'-UUCUCCGAA CGUGUCACGUTT-3').

Western blot analysis. Radio-immunoprecipitation assay (RIPA) lysis buffer (Sigma-Aldrich; Merck KGaA-Aldrich; Merck KGaA) was used to extract the protein of serum and cells. Total protein concentration was quantified using a BCA protein quantification kit (Invitrogen; Thermo Fisher Scientific, Inc.).

The extracted total protein (20 μg) was separated through the sodium dodecyl sulphate-polyacrylamide gel electrophoresis by 10% running gel and 5% stacking gel. Then, the separated protein was transferred onto PVDF membranes. Following immersion in TBST buffer with 5% skimmed milk at room temperature for 1 h, the PVDF membranes were incubated with primary antibodies overnight at 4˚C. The primary antibodies were obtained from Abcam or Santa Cruz Biotechnology, including anti-CD9 (cat. no. ab92726, 1:100), anti-CD63 (cat. no. ab59479, 1:200), anti-B cell lymphoma 2 (Bcl-2; cat. no. ab182858, 1:200), anti-cleaved caspase-3 (cat. no. ab32042, 1:500), anti-Bcl-2-associated X (Bax; cat. no. ab32503, 1:1,000), anti-GAPDH (cat. no. ab8245, 1:1,000), anti-interleukin (IL)-6 (cat. no. ab6672, 1:500), anti-IL-1β (cat. no. ab9722, 1:250), anti-TNF-α (sc-52B83, 1:500), anti-HMGB1 (cat. no. ab79823, 1:1,000), anti-Toll-like receptor 4 (TLR4; cat. no. ab13556, 1:500), anti-aggrecan (cat. no. ab3778, 1:100), anti-matrix metallopeptidase 13 (MMP13; cat. no. ab84594, 1:200), anti-NF-κB p65 (cat. no. ab16502, 1:200), anti-phosphorylated (p)-p65 (cat. no. ab97726, 1:1,000), anti-nuclear factor κ-B (NF-κB) inhibitor α (IκBα; cat. no. ab7217, 1:1,000) and anti-p-IκB-α (cat. no. ab24783, 1:1,000). Then the membranes were incubated with the secondary antibody goat anti-mouse IgG (cat. no. ab205719, 1:10,000) or anti-rabbit IgG (cat. no. ab205718, 1:1,000, both from Abcam) at room temperature for 1 h. GAPDH was used as a loading control. The Immobilon Western Chemiluminescent HRP Substrate (EMD Millipore) was used to visualize the protein bands. Quantification of protein bands was performed using ImageJ software 1.50 (National Institutes of Health).

Reverse transcription-quantitative (RT-q) PCR. Total RNA of the exosomes, serum and cells ($1x10^6$) was extracted through TRIzol® reagent (Thermo Fisher Scientific, Inc.). The first-strand complementary DNA (cDNA) for PVT1 and HMGB1 was generated through a Moloney Murine Leukemia Virus (M-MLV) First Strand kit (Thermo Fisher Scientific, Inc.). The first-strand cDNA for miR-93-5p was synthesized using MiRNA Reverse Transcription kit (Thermo Fisher Scientific, Inc.). RNA extraction and cDNA synthesis were performed in accordance with the manufacturer's protocols. RT-qPCR was conducted using SYBR Green PCR Master mixes (Thermo Fisher Scientific, Inc.) in a reaction volume of 20 μl (10 μl SYBR Premix Ex Taq II, 6 μl ddH2O, 2 μl cDNA, and 2 μl primer) with the following reaction program: 95˚C for 30 sec, followed by 40 cycles of 95˚C for 5 sec and 60˚C for 20 sec. The primers used were: PVT1: 5'-TTGGCACATACA GCCATCAT-3' forward (F) and 5'-GCAGTAAAAGGGGAA CACCA-3' reverse (R); HMGB1: 5'-CTCAGAGAGGTGGAA GACCATGT-3' (F) and 5'-GGGATGTAGGTTTTCATTTCT CTTTC-3' (R); GAPDH: 5'-GACTCCACTCACGGCAAA TTCA-3' (F) and 5'-TCGCTCCTGGAAGATGGTGAT-3' (R) miR-93-5p: 5'-GCCGCCAAAGTGCTGTTC-3' (F) and 5'-CAGAGCAGGGTCCGAGGTA-3' (R); as well as U6 small nuclear (sn) RNA: 5'-GCTCGCTTCGGCAGCACA-3' (F) and 5'-GAGGTATTCGCACCAGAGGA-3' (R). The expression of PVT1, HMGB1 and miR-93-5p was calculated by the $2^{-\Delta\Delta Cq}$ method (28) and GAPDH or U6 snRNA was used as an internal control. All RT-qPCR reactions were performed in triplicate.

Cell viability assay. Cell Counting Kit-8 (CCK-8) (Dojindo Molecular Technologies, Inc.) was applied to assess the viability of cells according to the manufacturer's protocol. In short, C28/I2 cells ($5x10^3$ cells/well) were treated with LPS (1, 5 and 10 μg/ml) for 48 h or LPS-stimulated C28/I2 cells transfected with oligonucleotides or plasmids were cultured for 48 h. Then, CCK-8 (10 μl) reagent was supplemented to each well and incubated at 37˚C for 2 h. A microplate absorbance reader (Thermo Fisher Scientific, Inc.) was used for the evaluation of the color reaction at 450 nm.

Flow cytometric assay. An Annexin V-fluorescein isothiocyanate (FITC)/propidium iodide (PI) apoptosis detection kit (Sigma-Aldrich; Merck KGaA) was employed to assess the apoptosis rate of cells according to the manufacturer's protocol. In brief, the C28/I2 cells were treated in the same manner as for the cell viability assay. Following washing, treated C28/I2 cells ($1x10^5$) were resuspended in binding buffer. Annexin V-FITC (5 μl) and PI (10 μl) were added to the binding buffer and incubated at room temperature for 15 min in the dark. A FACScan flow cytometer (BD Biosciences) with CellQuest software (version 5.1, BD Biosciences) was used to analyze the apoptosis rate of treated C28/I2 cells.

Enzyme-linked immunosorbent assay (ELISA). The levels of inflammatory cytokines IL-6, IL-1β and TNF-α in the supernatant of treated-C28/I2 cells were analyzed with human IL-1β (cat. no. SLB50)/IL-6 (cat. no. S6050)/TNF-α (cat. no. STA00D) Quantikine ELISA kits (R&D Systems Europe, Ltd.).

Dual-luciferase reporter assay. StarBase v2.0 (http://starbase.sysu.edu.cn/) was employed to predict the binding sites between PVT1 or HMGB1 and miR-93-5p. Then, the sequences of wild-type (WT) PVT1 (with predicted miR-93-5p binding sites) and mutant (MUT) PVT1 were amplified and inserted into the psiCHECK-2 vector (Promega Corporation) to establish the luciferase reporter vectors WT-PVT1 and MUT-PVT1 for the verification of the binding sites between PVT1 and miR-93-5p. The same method was used to construct the reporter vectors HMGB1 3' untranslated region (UTR)-WT and HMGB1 3'UTR-MUT for the confirmation of the binding sites between HMGB1 and miR-93-5p. C28/I2 cells were cotransfected miR-NC (30 nM) or miR-93-5p (30 nM) and a luciferase reporter vector (100 ng) Lipofectamine® 3000 reagent (Invitrogen; Thermo Fisher Scientific, Inc.). After transfection for 48 h, the luciferase activities of the luciferase reporter vectors were evaluated with dual-luciferase reporter assay kit (Promega Corporation). Relative *Renilla* luciferase activity was normalized to that of firefly luciferase.

Statistical analysis. SPSS 20.0 software (IBM Corp.) and GraphPad Prism 5.0 (GraphPad Software, Inc.) were used for statistical analysis. The data in the present study were derived from ≥3 independent experiments. Data are presented as the mean ± standard deviation. Unpaired Student's t-test or one-way variance analysis (ANOVA) with Tukey's post hoc test was employed. Pearson's correlation analysis method was used to assess the relationship between miR-93-5p and PVT1 as well as HMGB1 and miR-93-5p expression in the serum

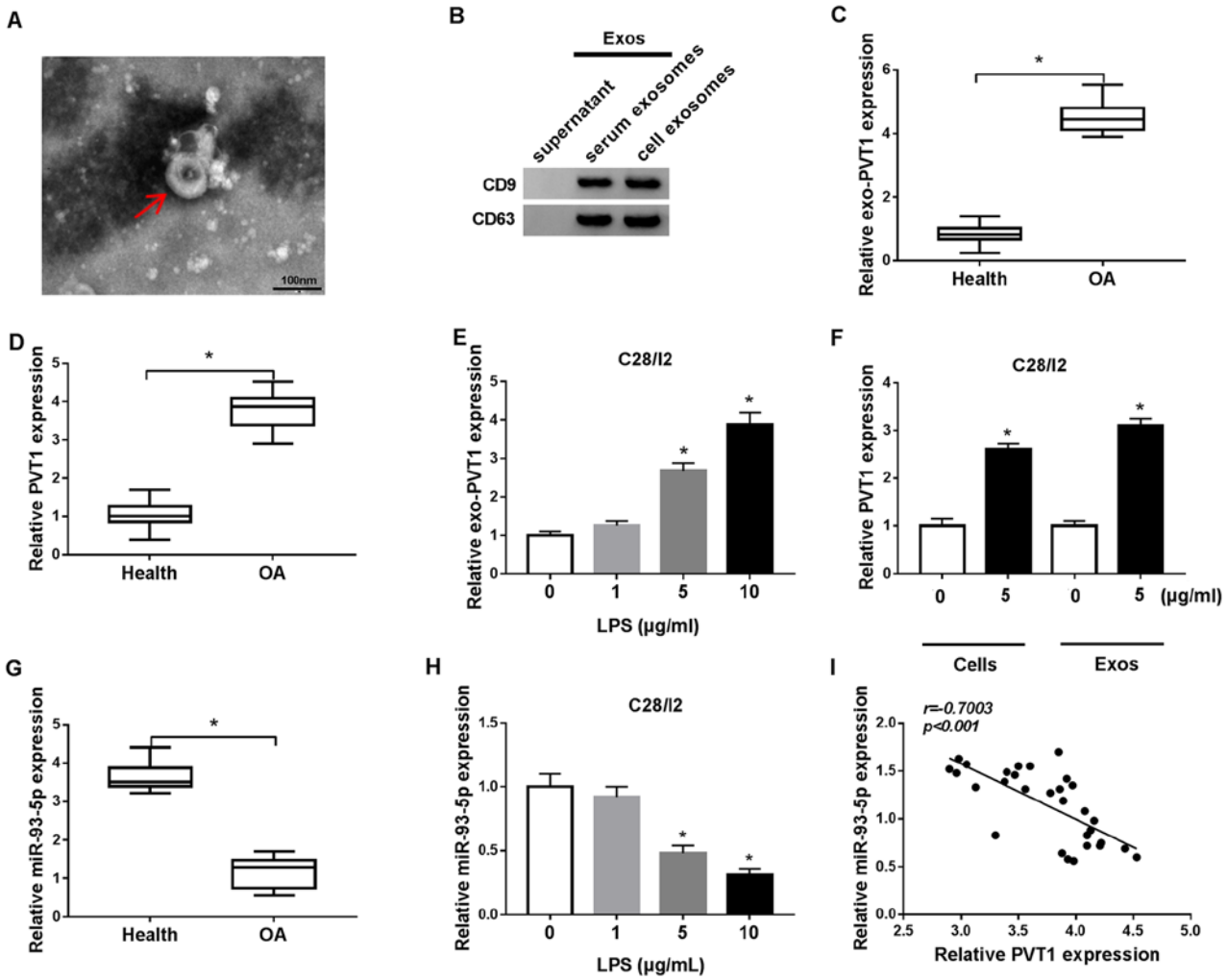

Figure 1. Expression patterns of exosomal PVT1 and miR-93-5p in the serum of osteoarthritis patients and LPS-stimulated C28/I2 cells. (A) TEM image of the exosomes released by the serum of osteoarthritis patients and C28/I2 cells (magnification, x100,000). (B) Exosomal protein markers (CD9 and CD63) were detected by western blot analysis from purified exosomes and exosome-depleted supernatant. The levels of (C) PVT1 and (D) exosomal PVT1 in the serum of osteoarthritis patients and healthy volunteers were detected using RT-qPCR. (E) The level of exosomal PVT1 in C28/I2 cells treated with various concentrations of LPS (0, 1, 5 and 10 μg/ml) was assessed by RT-qPCR. (F) Effect of the exosomes of 5 μg/ml LPS-stimulated C28/I2 cells and the serum of osteoarthritis patients on the expression of PVT1 of C28/I2 cells was analyzed via RT-qPCR. (G) The expression of miR-93-5p in the serum of osteoarthritis patients was examined by RT-qPCR. (H) Effects of various concentrations of LPS on miR-93-5p expression level of C28/I2 cells were analyzed through RT-qPCR. (I) Pearson correlation analysis revealed a correlation between miR-93-5p and PVT1 in the serum of patients with osteoarthritis. *P<0.05. PVT1, plasmacytoma variant translocation 1; miR, microRNA; LPS, lipopolysaccharide; TEM, transmission electron microscopy; RT-qPCR, reverse transcription-quantitative PCR.

of osteoarthritis patients. P<0.05 was considered to indicate a statistically significant difference.

Results

Expression of PVT1, exosomal PVT1, miR-93-5p in the serum of osteoarthritis patients and LPS-stimulated C28/I2 cells. Exosomes were extracted from C28/I2 cells and from the serum of patients with osteoarthritis to analyze exosome-encapsulated PVT1 in osteoarthritis. The exosomes were circular in shape and 40-100 nm in the C28/I2 cells and the serum of osteoarthritis patients and healthy volunteers (Fig. 1A). Western blot analysis demonstrated that the exosome marker proteins CD9 and CD63 were present in the exosomes of the C28/I2 cells and the serum of osteoarthritis patients (Fig. 1B). RT-qPCR demonstrated that PVT1 was significantly upregulated in exosomes of the serum of osteoarthritis patients when compared with the serum of healthy volunteers (Fig. 1C). In addition, PVT1 was significantly upregulated in the serum of osteoarthritis patients compared with healthy volunteers (Fig. 1D). LPS (1, 5 and 10 μg/ml) was used to treat C28/I2 cells for the construction of the osteoarthritis status *in vitro*. It was determined that the expression of PVT1 was significantly enhanced in exosomes of 5 and 10 μg/ml LPS-stimulated C28/I2 cells (Fig. 1E). Furthermore, it was identified that the exosomes of 5 μg/ml LPS-stimulated C28/I2 cells and the serum of osteoarthritis patients could increase the expression of exosomal PVT1 in C28/I2 cells (Fig. 1F).

miR-93-5p in the serum of patients with osteoarthritis was decreased compared with the serum of healthy volunteers (Fig. 1G). In addition, miR-93-5p was significantly downregulated in LPS (5 and 10 μg/ml)-treated C28/I2 cells (Fig. 1H). Pearson correlation analysis demonstrated that the expression of miR-93-5p and PVT1 was negatively correlated in the

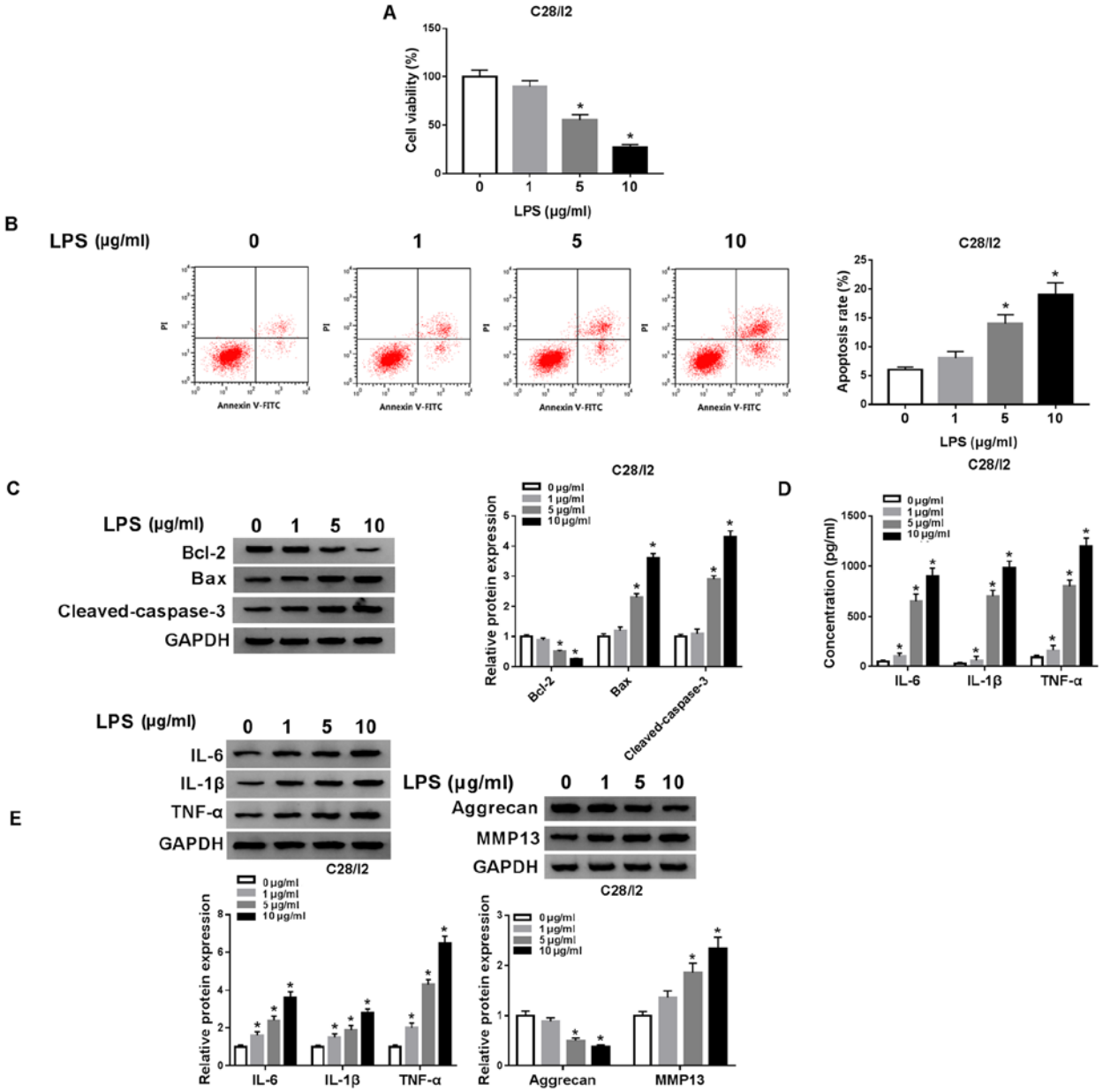

Figure 2. Effects of LPS on viability and induced cell apoptosis, inflammation responses and collagen degradation of C28/I2 cells. (A) Influence of various concentrations of LPS (0, 1, 5 and 10 μg/ml) on viability of C28/I2 cells as determined by CCK-8 assay. (B) The apoptosis of C28/I2 cells cultured in medium with various concentrations of LPS was detected by flow cytometry. (C) Western blot analysis was performed to assess the protein levels of Bcl-2, Bax and cleaved caspase-3 in the C28/I2 cells cultured in medium with various concentrations of LPS. (D) The levels of IL-6, IL-1β and TNF-α in C28/I2 cells stimulated with various concentrations of LPS were assessed using ELISA. (E) The protein levels of IL-6, IL-1β, TNF-α, aggrecan and MMP13 in C28/ I2 cells treated with various concentrations of LPS were assessed by western blot analysis. *P<0.05. LPS, lipopolysaccharide; IL, interleukin; MMP, matrix metallopeptidase.

serum of patients with osteoarthritis (Fig. 1I). Collectively, these results indicated that the upregulation of PVT1 mediated by exosomes and the reduction of miR-93-5p may be associated with the pathogenesis of osteoarthritis.

LPS accelerates cell apoptosis and inflammation responses and restrains cell viability in C28/I2 cells. The influence of LPS on the viability, apoptosis and inflammation responses of C28/I2 cells was investigated. A CCK-8 assay demonstrated that the viability of C28/I2 cells was significantly suppressed with increased concentration of LPS (Fig. 2A). Flow cytometry revealed that the apoptosis rate of C28/I2 cells was significantly increased with increased concentration of LPS (Fig. 2B). The levels of apoptosis-related proteins (Bcl-2, Bax and cleaved caspase-3) in LPS-stimulated C28/I2 cells were analyzed with western blot analysis. With increased concentration of LPS, Bcl-2 protein level in C28/I2 cells was reduced, while Bax and cleaved caspase-3 protein levels were increased (Fig. 2C). The levels of inflammatory cytokines IL-6, IL-1β and TNF-α in the supernatant of LPS-stimulated C28/I2 cells were measured using ELISA. The results demonstrated that the levels of IL-6, IL-1β and TNF-α were increased in the supernatant of C28/I2 cells with increased concentration of LPS (Fig. 2D). LPS increased the protein levels of IL-6, IL-1β and TNF-α in

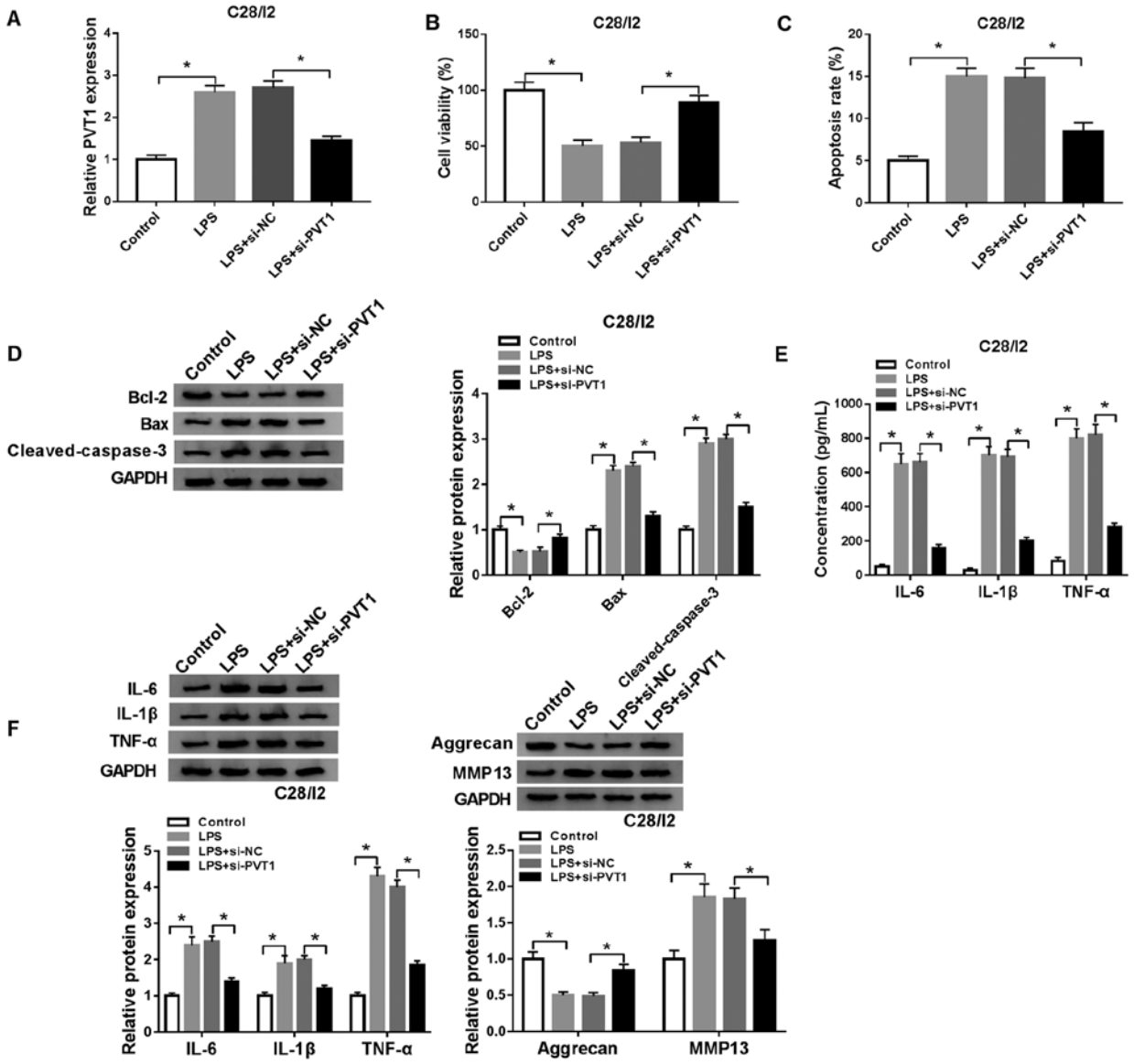

Figure 3. Effects of PVT1 depletion on viability, apoptosis, inflammation responses and collagen degradation in LPS-stimulated C28/I2 cells. LPS-stimulated C28/I2 cells were transfected with si-NC or si-PVT1. (A) RT-qPCR was employed to analyze the expression of PVT1 in LPS-stimulated C28/I2 cells. (B) Effect of PVT1 inhibition on cell viability in LPS-stimulated C28/I2 cells was analyzed using a CCK-8 assay. (C) Influence of PVT1 inhibition on the apoptosis rate of LPS-stimulated C28/I2 cells as determined using flow cytometry. (D) Effects of PVT1 inhibition on Bcl-2, Bax and cleaved caspase-3 protein expression levels were evaluated with western blot analysis. (E) ELISA was used to analyze the effects of PVT1 silencing on IL-6, IL-1β and TNF-α expression levels in the supernatant of LPS-stimulated C28/I2 cells. (F) Western blot analysis was performed to assess the influence of PVT1 downregulation on the protein levels of IL-6, IL-1β, TNF-α, aggrecan and MMP13 in LPS-stimulated C28/I2 cells. *P<0.05. PVT1, plasmacytoma variant translocation 1; LPS, lipopolysaccharide; si, short interfering RNA; NC, negative control; RT-qPCR, reverse transcription-quantitative PCR; IL, interleukin; MMP, matrix metallopeptidase.

C28/I2 cells in a concentration-dependent manner (Fig. 2E). Aggrecan levels were reduced while MMP13 levels were increased in C28/I2 cells with increased concentration of LPS, indicating that LPS treatment induced collagen degradation in C28/I2 cells (Fig. 2E). Collectively, these findings demonstrated that LPS could induce cell apoptosis and inflammation responses and inhibit cell viability in C28/I2 cells.

Depletion of PVT1 overturns LPS-mediated viability, apoptosis and inflammation responses and collagen degradation of C28/I2 cells. To investigate the function of PVT1 in osteoarthritis, a function-loss-experiment was performed in C28/I2 cells treated with LPS (5 μg/ml) for 48 h. The results demonstrated that PVT1 expression was significantly increased in C28/I2 cells following exosome treatment. In addition, the upregulation of PVT1 in C28/I2 cells caused by exosome treatment was reversed after si-PVT1 transfection (Fig. S1). The transfection of si-PVT1 abolished the upregulation of PVT1 in LPS-stimulated C28/I2 cells compared with the si-NC group (Fig. 3A). A CCK-8 assay demonstrated that PVT1 downregulation reversed the suppressive influence of LPS on the viability of C28/I2 cells (Fig. 3B). The increase of apoptosis in LPS-treated C28/I2 cells was reversed by the downregulation of PVT1 (Fig. 3C). In addition, the enhancement of Bax and cleaved caspase-3 proteins and the decrease of Bcl-2 protein in LPS-induced C28/I2 cells were overturned by PVT1 inhibition (Fig. 3D). ELISA revealed that reduced PVT1 expression abrogated the increase in IL-6, IL-1β and TNF-α in C28/I2 cells treated with LPS (Fig. 3E). Western

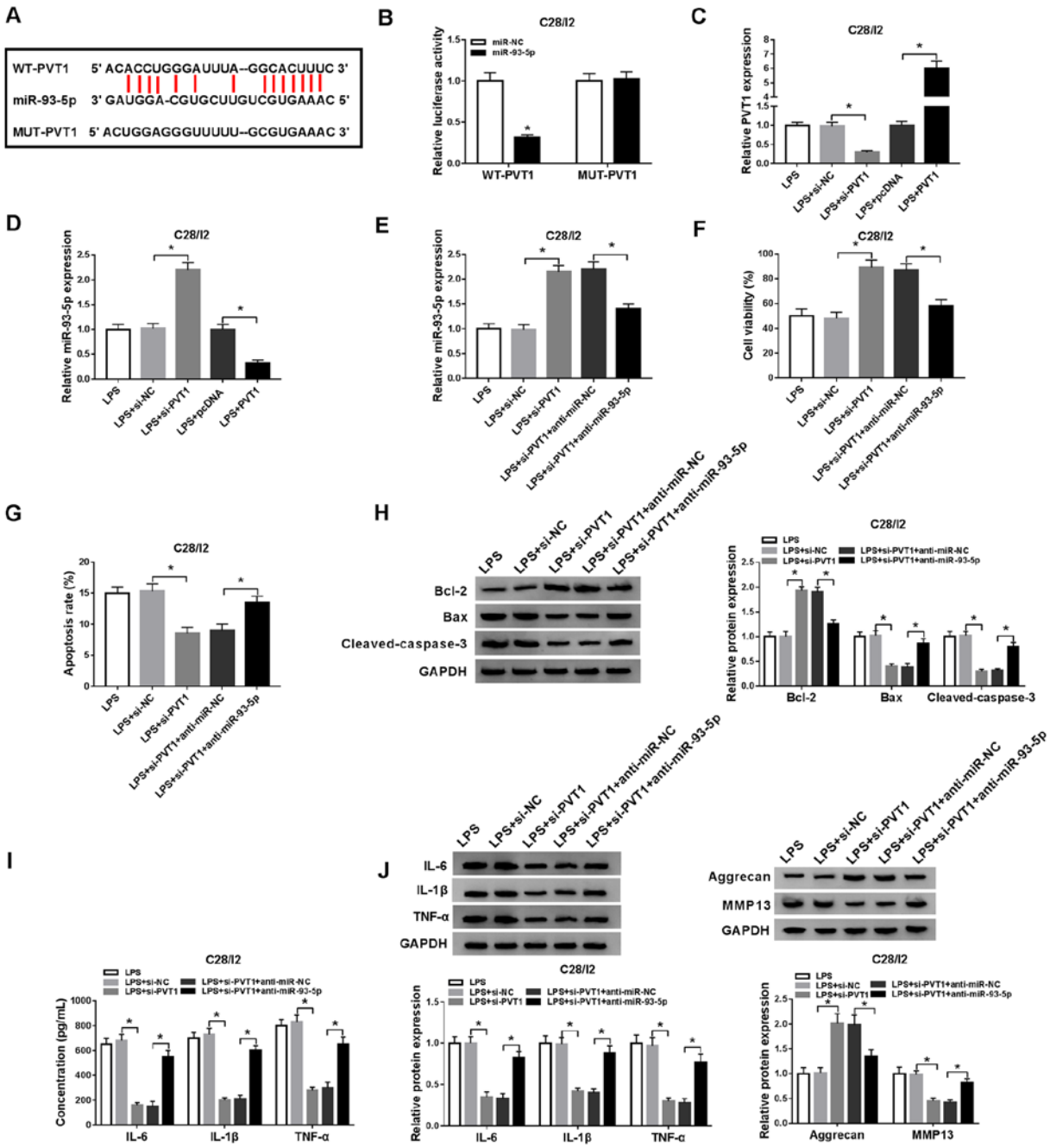

Figure 4. PVT1 performs its role through miR-93-5p in C28/I2 cells. (A) The binding sites of PVT1 in miR-93-5p were predicted using starBase v2.0. (B) The luciferase intensity in C28/I2 cells cotransfected WT-PVT1 or MUT-PVT1 and miR-NC or miR-93-5p were determined with dual-luciferase reporter assay. (C) RT-qPCR was performed to analyze PVT1 expression level in LPS-stimulated C28/I2 cells transfected with si-PVT1 or PVT1. (D) Effect of PVT1 on the expression of miR-93-5p was evaluated using RT-qPCR. LPS-stimulated C28/I2 cells were transfected with si-NC, si-PVT1, si-PVT1+anti-miR-NC, si-PVT1+anti-miR-93-5p. (E) Effect of miR-93-5p suppression on PVT1 knockdown-mediated miR-93-5p expression of LPS-stimulated C28/I2 cells was analyzed using RT-qPCR. (F) Effect of miR-93-5p inhibition on PVT1 downregulation-mediated viability of LPS-stimulated C28/I2 cells was determined via CCK-8 assay. (G) Flow cytometry was performed for the evaluation of the influence of miR-93-5p silencing on PVT1 inhibition-mediated apoptosis of LPS-stimulated C28/I2 cells. (H) Western blot analysis was performed to detect the protein levels of Bcl-2, Bax and cleaved caspase-3 in LPS-stimulated C28/ I2 cells. (I) The levels of IL-6, IL-1β and TNF-α in LPS-stimulated C28/I2 cells were measured using ELISA. (J) The protein levels of IL-6, IL-1β, TNF-α, aggrecan and MMP13 in LPS-stimulated C28/I2 cells were explored using western blot analysis. *P<0.05. PVT1, plasmacytoma variant translocation 1; miR, microRNA; WT, wild-type; MUT, mutant; RT-qPCR, reverse transcription-quantitative PCR; LPS, lipopolysaccharide; si, short interfering RNA; NC, negative control; IL, interleukin; MMP, matrix metallopeptidase.

blot analysis also demonstrated that PVT1 silencing reversed LPS-mediated effects on the protein levels of IL-6, IL-1β, TNF-α, aggrecan and MMP13 in C28/I2 cells (Fig. 3F). In brief, PVT1 downregulation abolished LPS-mediated viability, apoptosis, inflammation responses and collagen degradation in C28/I2 cells.

miR-93-5p acts as a target for PVT1. To understand the molecular mechanism of PVT1 in osteoarthritis, starBase v2.0 was used to predict the potential binding sites for PVT1. miR-93-5p was revealed to be a possible target for PVT1 (Fig. 4A). Subsequently, the luciferase reporter vectors WT-PVT1 and MUT-PVT1 were constructed to verify the potential binding

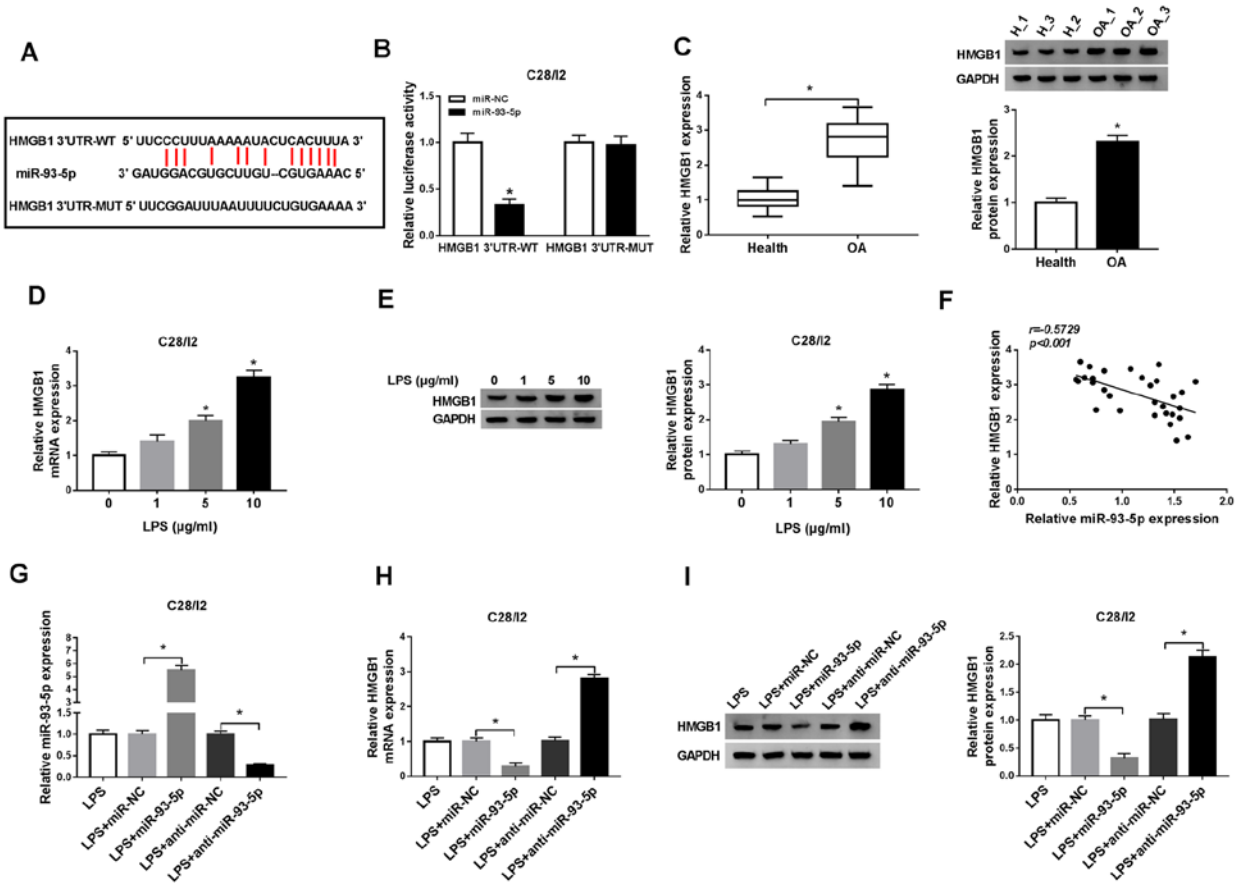

Figure 5. HMGB1 serves as a target for miR-93-5p. (A) miR-93-5p latent binding sites in HMGB1 as predicted by starBase v2.0. (B) Dual-luciferase reporter assay was performed to determine the luciferase intensity in C28/I2 cells cotransfected with HMGB1 3'UTR-WT or HMGB1 3'UTR-MUT and miR-NC or miR-93-5p. (C) RT-qPCR or western blot analysis was employed to evaluate the levels of HMGB1 mRNA and protein in the serum of osteoarthritis patients. The expression levels of HMGB1 mRNA and protein in C28/I2 cells treated with LPS (0, 1, 5 and 10 μg/ml) were measured using (D) RT-qPCR or (E) western blot analysis. (F) The correlation between HMGB1 and miR-93-5p in the serum of osteoarthritis patients was analyzed via Pearson correlation analysis. (G) The effect of miR-93-5p on the expression of miR-93-5p of LPS-stimulated C28/I2 cells was assessed by RT-qPCR. The effect of miR-93-5p on the mRNA and protein levels of HMGB1 miR-93-5p of LPS-stimulated C28/I2 cells was determined by (H) RT-qPCR or (I) western blot analysis. *P<0.05. HMGB1, high mobility groupprotein B1; UTR, untranslated region; WT, wild-type; MUT, mutant; miR, microRNA; NC, negative control; RT-qPCR, reverse transcription-quantitative PCR; LPS, lipopolysaccharide.

sites between PVT1 and miR-93-5p. Dual-luciferase reporter assay demonstrated that miR-93-5p introduction suppressed the luciferase activity of WT-PVT1 when compared with the miR-NC, while no significant difference was observed in luciferase activity between the miR-NC and MUT-PVT1 groups (Fig. 4B). RT-qPCR demonstrated that PVT1 expression level was decreased in LPS-stimulated C28/I2 cells transfected with si-PVT1, but the expression of PVT1 was enhanced in LPS-stimulated C28/I2 cells transfected with PVT1 (Fig. 4C). Decreased PVT1 expression effectively increased miR-93-5p expression in LPS-stimulated C28/I2 cells, whereas increased levels of PVT1 suppressed miR-93-5p expression in LPS-stimulated C28/I2 cells (Fig. 4D). The introduction of anti-miR-93-5p overturned PVT1 downregulation-mediated enhancement of miR-93-5p in LPS-stimulated C28/I2 cells (Fig. 4E). Whether PVT1 exerted its function via miR-93-5p in LPS-stimulated C28/I2 cells was then investigated. A CCK-8 assay demonstrated that the promotion of proliferation of LPS-stimulated C28/I2 cells caused by PVT1 silencing was reversed by the inhibition of miR-93-5p (Fig. 4F). miR-93-5p silencing overturned the suppression of apoptosis in LPS-stimulated C28/I2 cells induced by PVT1 knockdown (Fig. 4G). Western blot analysis revealed that the downregulation of miR-93-5p abrogated PVT1 reduction-mediated protein levels of Bcl-2, Bax and cleaved caspase-3 of LPS-stimulated C28/I2 cells (Fig. 4H). ELISA revealed that miR-93-5p reduction reversed the suppression of IL-6, IL-1β and TNF-α in LPS-stimulated C28/I2 cells induced by PVT1 downregulation (Fig. 4I). Western blot analysis also revealed that downregulated miR-93-5p expression reversed the PVT1 inhibition-mediated influence on the protein levels of IL-6, IL-1β, TNF-α, aggrecan and MMP13 in C28/I2 cells following LPS treatment (Fig. 4J). Therefore, these data indicated that PVT1 mediated cell viability, apoptosis, inflammation responses and collagen degradation in LPS-stimulated C28/I2 cells via miR-93-5p.

HMGB1 serves as a target for miR-93-5p. To further investigate the molecular mechanism of miR-93-5p in osteoarthritis, the latent target for miR-93-5p was explored in starBase v2.0. As illustrated in Fig. 5A, miR-93-5p possessed latent binding sites in HMGB1. The luciferase reporter vectors HMGB1 3'UTR-WT and HMGB1 3'UTR-MUT were then established and a dual-luciferase reporter assay demonstrated a significant

suppression of luciferase activity of HMGB1 3'UTR-WT in C28/I2 cells transfected with miR-93-5p compared with the negative control group, while HMGB1 3'UTR-MUT luciferase activity was not noticeably altered (Fig. 5B). In addition, the mRNA and protein levels of HMGB1 were significantly upregulated in the serum of osteoarthritis patients (Fig. 5C). The mRNA and protein levels of HMGB1 were significantly increased in LPS (5 μg/ml)-treated C28/I2 cells, implying that HMGB1 may be associated with LPS-induced osteoarthritis (Fig. 5D and E). A negative correlation was observed between miR-93-5p and HMGB1 in the serum of osteoarthritis patients (Fig. 5F). The introduction of miR-93-5p significantly upregulated miR-93-5p in LPS-stimulated C28/I2 cells, whereas the introduction of anti-miR-93-5p downregulated miR-93-5p in LPS-stimulated C28/I2 cells (Fig. 5G). The mRNA and protein levels of HMGB1 were suppressed by miR-93-5p introduction in LPS-stimulated C28/I2 cells, while these effects were reversed by miR-93-5p silencing (Fig. 5H and I). These findings revealed that miR-93-5p negatively regulated the expression of HMGB1 in LPS-stimulated C28/I2 cells.

HMGB1 increase abolishes miR-93-5p overexpression-mediated viability, apoptosis, inflammation responses and collagen degradation of LPS-stimulated C28/I2 cells. To ascertain whether miR-93-5p-mediated viability, apoptosis and inflammation responses of LPS-stimulated C28/I2 cells were dependent on HMGB1, the expression of HMGB1 was explored in LPS-stimulated C28/I2 cells transfected with miR-NC, miR-93-5p, miR-93-5p+pcDNA or miR-93-5p+HMGB1. The results revealed that the mRNA and protein levels of HMGB1 were inhibited by miR-93-5p upregulation in LPS-stimulated C28/I2 cells, but this suppression was overturned by the addition of HMGB1 (Fig. 6A and B). A CCK-8 assay revealed that the enhanced miR-93-5p expression resulted in increased viability of LPS-stimulated C28/I2 cells, whereas this influence was reversed by the upregulation of HMGB1 (Fig. 6C). Flow cytometry revealed that miR-93-5p overexpression served a repressive role in the apoptosis of LPS-stimulated C28/I2 cells, while this influence was restored by upregulation of HMGB1 expression (Fig. 6D). Overexpression of HMGB1 abolished the decrease of Bax and cleaved caspase-3 and the upregulation of Bcl-2 caused by miR-93-5p increase in LPS-stimulated C28/I2 cells (Fig. 6E). In addition, the downregulation of IL-6, IL-1β, TNF-α and MMP13 and the upregulation of aggrecan in LPS-stimulated C28/I2 cells caused by miR-93-5p upregulation were overturned by HMGB1 expression (Fig. 6F and G). PVT1 depletion significantly downregulated the mRNA and protein levels of HMGB1 in LPS-stimulated C28/I2 cells, but this reduction was recovered by the inhibition of miR-93-5p (Fig. 6H and I). The aforementioned data indicated that miR-93-5p mediated cell viability, apoptosis, inflammation responses and collagen degradation in LPS-stimulated C28/I2 cells through HMGB1.

PVT1 silencing blocks the TLR4/NF-κB pathway through the miR-93-5p/HMGB1 axis. The TLR4/NF-κB pathway is associated with the secretion of pro-inflammatory cytokines (29). Hence, the present study investigated whether the TLR4/NF-κB pathway was involved in PVT1-mediated cell viability, apoptosis and inflammation responses in LPS-stimulated C28/I2 cells. Western blot analysis demonstrated that LPS treatment promoted the protein levels of p-p65, TLR4 and p-IκB-α in C28/I2 cells (Fig. 7A). Inhibition of PVT1 reversed the increase of TLR4, p-p65 and p-IκB-α proteins in C28/I2 cells induced by LPS. However, inhibition of miR-93-5p and HMGB1 upregulation abolished the suppressive impact of PVT1 suppression on p-p65, TLR4 and p-IκB-α protein expression levels in LPS-stimulated C28/I2 cells (Fig. 7B). Additionally, the data indicated that LPS-induced PVT1 accelerated osteoarthritis by activating the TLR4/NF-κB pathway through the miR-93-5p/HMGB1 axis in C28/I2 cells (Fig. 7C). These findings indicated that PVT1 regulated the TLR4/NF-κB pathway through the miR-93-5p/HMGB1 axis.

Discussion

Osteoarthritis mainly affects the health of middle-aged and elderly people and its clinical manifestations include joint pain, deformity and dysfunction (30). LPS is a key pro-inflammatory factor associated with the onset of osteoarthritis (31). Studies have revealed that LPS can be used to construct a cell injury model *in vitro* (32-34). The present study used 5 μg/ml LPS to construct a cell injury model *in vitro*. Increasing evidence emphasizes the association of lncRNAs with the progression of osteoarthritis and the probability that lncRNAs function as therapeutic targets and biomarkers (8,9,35,36). Exosomes can transport their loaded nucleic acids and proteins to recipient cells, thereby playing a central role in cell-to-cell communication (37). The present study revealed that exosomal PVT1 was upregulated in the serum of osteoarthritis patients and LPS-stimulated C28/I2 cells. In addition, PVT1 was upregulated in the serum of osteoarthritis patients compared with the healthy volunteers. Notably, the exosomes of the serum of osteoarthritis patients and LPS-stimulated C28/I2 cells could enhance the expression of PVT1 in C28/I2 cells. Li *et al* (13) revealed that PVT1 enhancement facilitates cell apoptosis in chondrocytes in osteoarthritis. A previous study stated that increased PVT1 expression expedites inflammation and aberrant metabolic dysfunction in IL-β-induced chondrocytes (38). PVT1 is associated with the development of hyperglycemia-induced collagen degradation in chondrocytes (36). In the present study, inhibition of PVT1 reversed the decrease of viability and the increase of apoptosis, inflammation responses and collagen degradation in C28/I2 cells induced by LPS, implying that PVT1 acted as an unfavorable factor in osteoarthritis.

Previous studies suggest that PVT1 can be used as a sponge for miRNAs to participate in the development of osteoarthritis (13,38,39). miR-93-5p-containing exosomes attenuated the myocardial injury caused by acute myocardial damage (40). In addition, miR-93-5p was revealed to reverse the inflammatory and antiproliferative processes of neodymium oxide-induced human bronchial epithelial cell lines caused by circular RNA 0039411 (19). Xue *et al* (20) noted that miR-93-5p was decreased in IL-β-induced chondrocytes and human and rat osteoarthritis-affected cartilage and that introduction of miR-93-5p suppressed cell apoptosis, increased cell viability and maintained cell metabolism balance in IL-β-induced chondrocytes. In the present study, miR-93-5p

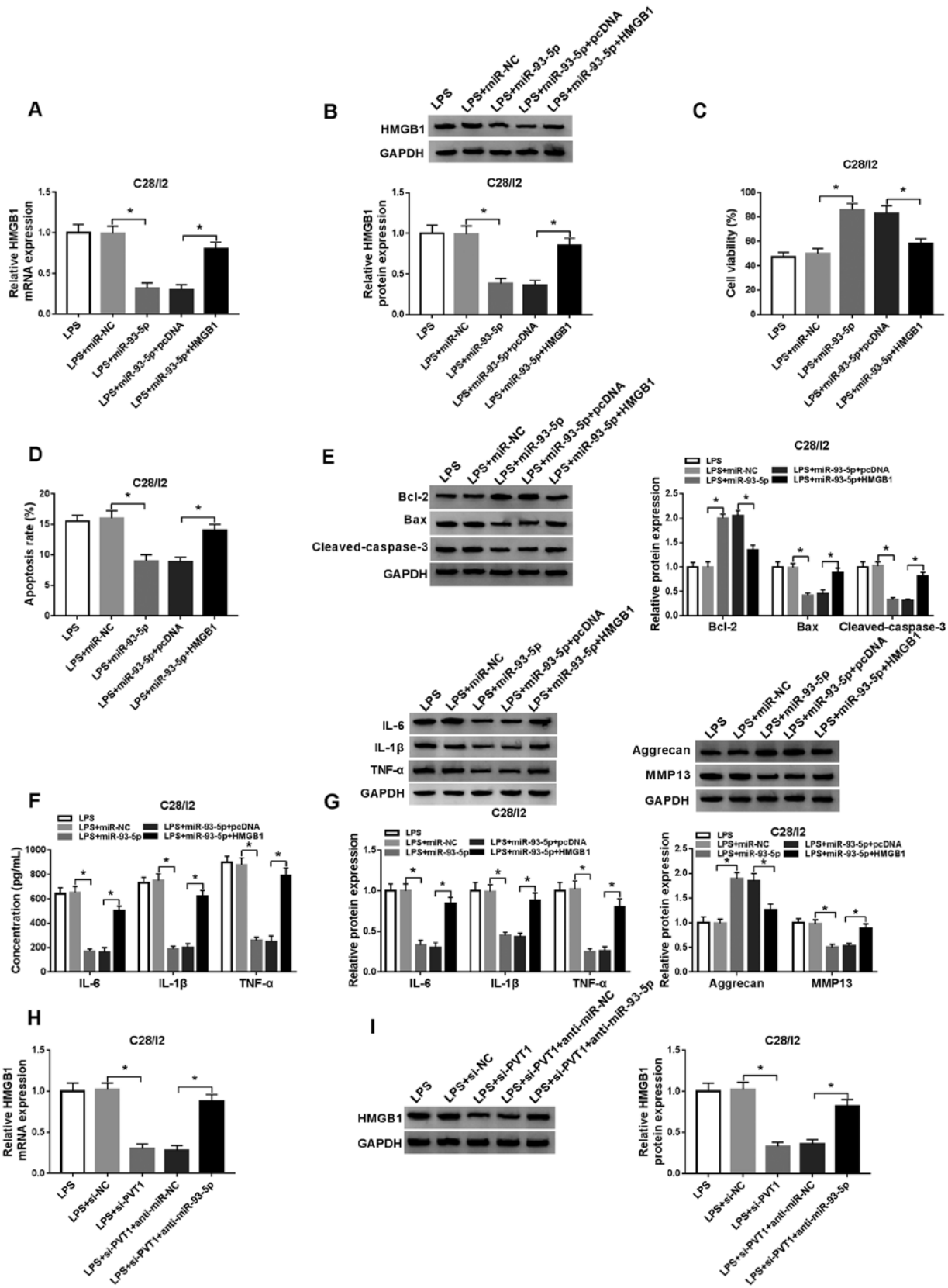

Figure 6. miR-93-5p exerts its function in LPS-stimulated C28/I2 cells through HMGB1. LPS-stimulated C28/I2 cells were transfected with miR-NC, miR-93-5p, miR-93-5p+pcDNA or miR-93-5p+HMGB1. The mRNA and protein expression levels of HMGB1 in LPS-stimulated C28/I2 cells were assessed through (A) RT-qPCR or (B) western blot analysis. (C) A CCK-8 assay was performed to determine the viability of LPS-stimulated C28/I2 cells. (D) The apoptosis of LPS-stimulated C28/I2 cells was detected by flow cytometry. (E) The protein levels of Bcl-2, Bax and cleaved caspase-3 in LPS-stimulated C28/I2 cells were evaluated by western blot analysis. (F) ELISA was applied to analyze the levels of IL-6, IL-1β and TNF-α in LPS-stimulated C28/I2 cells. (G) Western blot analysis was performed to assess the protein levels of IL-6, IL-1β, TNF-α, aggrecan and MMP13 in the LPS-stimulated C28/I2 cells. (H) RT-qPCR or (I) western blot analysis was employed to detect HMGB1 mRNA and protein expression levels in LPS-stimulated C28/I2 cells transfected with si-NC, si-PVT1, si-PVT1+anti-miR-NC and si-PVT1+anti-miR-93-5p. *P<0.05. miR, microRNA; LPS, lipopolysaccharide; HMGB1, high mobility groupprotein B1; NC, negative control; RT-qPCR, reverse transcription-quantitative PCR; IL, interleukin; MMP, matrix metallopeptidase; si, short interfering RNA.

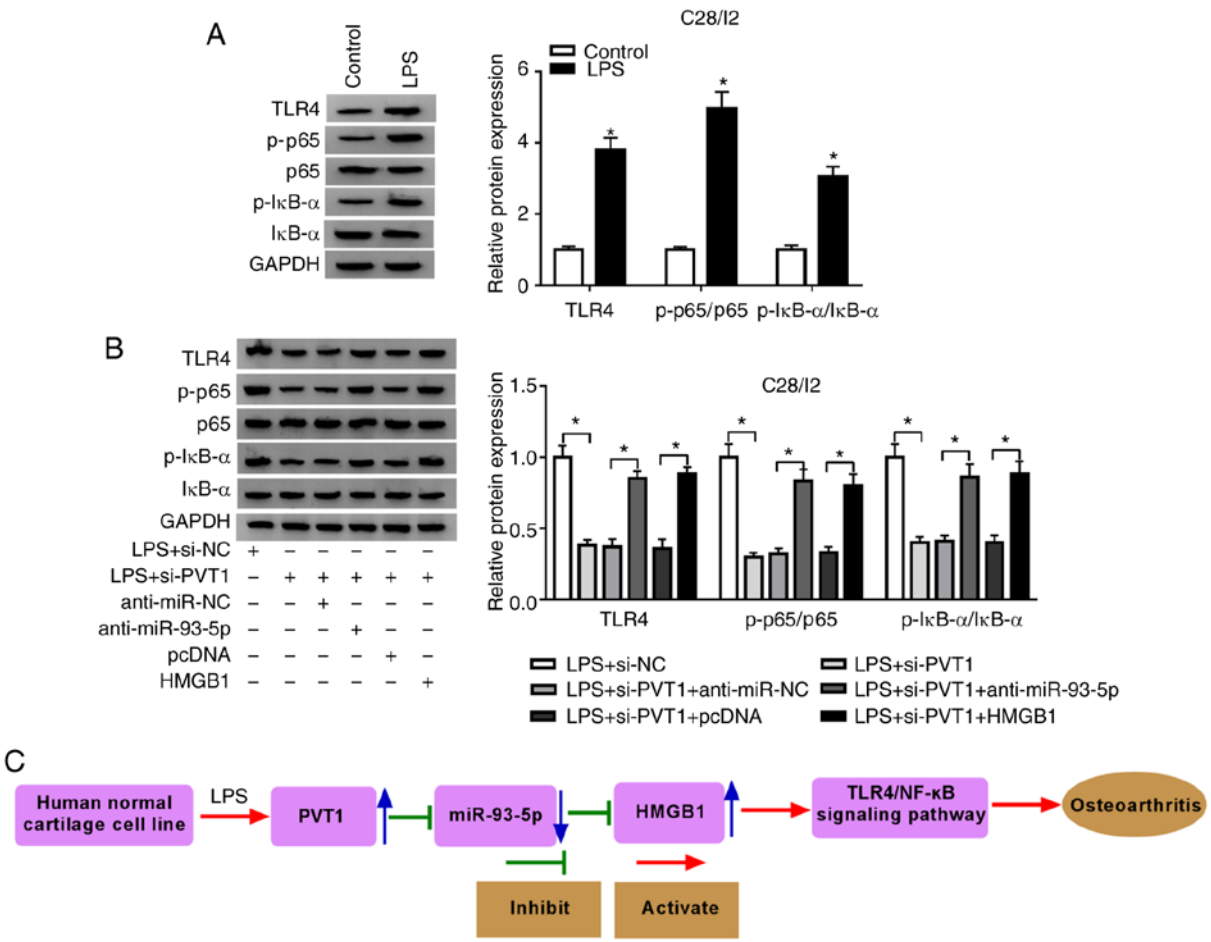

Figure 7. PVT1 modulates the TLR4/NF-κB pathway via the miR-93-5p/HMGB1 axis. (A) Effects of LPS on the expression of TLR4, p-p65 and p-IκB-α proteins of C28/I2 cells were determined with western blot analysis. (B) The expression of TLR4, p-p65 and p-IκB-α proteins in LPS-stimulated C28/I2 cells transfected with si-NC, si-PVT1, si-PVT1+anti-miR-NC, si-PVT1+anti-miR-93-5p, si-PVT1+pcDNA, or si-PVT1+anti-HMGB1. (C) The schematic presentation of the LPS/PVT1/miR-93-5p/HMGB1 axis in osteoarthritis. *P<0.05. PVT1, plasmacytoma variant translocation 1; TLR4,Toll-like receptor 4; miR, microRNA; HMGB1, high mobility groupprotein B1; LPS, lipopolysaccharide; p-, phosphorylated; IκBα, NF-κB inhibitor α; si, short interfering RNA; NC, negative control.

was downregulated in the serum of osteoarthritis patients and LPS-stimulated C28/I2 cells. Furthermore, miR-93-5p was a target of PVT1. Downregulation of miR-93-5p abolished PVT1 silencing-mediated viability, apoptosis, inflammation responses and collagen degradation of LPS-stimulated C28/I2 cells. These data implied that PVT1 mediated cell viability, apoptosis and inflammation responses in osteoarthritis through miR-93-5p.

HMGB1 is a member of the damage-associated molecular patterns (41). It is released from damaged or dead cells during tissue damage, necrosis, inflammation and hypoxia, resulting in a sustained inflammatory environment (42). The HMGB1-LPS complex accelerates the transformation of osteoarthritis synovial fibroblasts into the synovial fibroblast-like phenotype of rheumatoid arthritis (43). HMGB1 has been revealed to promote cell apoptosis, NF-κB and the production of IL-6, IL-1β and TNF-α in LPS-induced chondrocytes (44). In addition, necrostatin-1 has been revealed to ameliorate IL-1β-induced apoptosis and trauma-induced mouse osteoarthritis in primary mouse chondrocytes by inhibiting HMGB1/TLR4/SDF-1 (45). Inhibition of the transcriptional activity of HMGB1 and the NF-κB pathway by BRD4 silencing can attenuate chondrocyte inflammation and catabolism (46). In the present study, HMGB1 was enhanced in the serum of osteoarthritis patients and LPS-stimulated C28/I2 cells. Overexpression of HMGB1 abolished the decrease of viability and the increase of apoptosis, inflammation responses and collagen degradation in LPS-stimulated C28/I2 cells caused by miR-93-5p upregulation. In addition, PVT1 inhibition could block the HMGB1/TLR4/NF-κB pathway through miR-93-5p. Therefore, the present study indicated that PVT1 inhibition alleviated LPS-induced damage in osteoarthritis by blocking the HMGB1/TLR4/NF-κB pathway through miR-93-5p.

In summary, PVT1 was upregulated in serum and serum exosomes of osteoarthritis patients, as well as LPS-stimulated C28/I2 cells. PVT1 inhibition enhanced viability and suppressed apoptosis, inflammation responses and collagen degradation of LPS-stimulated C28/I2 cells. Therefore, exosome-mediated PVT1 regulated LPS-induced osteoarthritis progression by modulating the HMGB1/TLR4/NF-κB pathway via miR-93-5p. The present study aids to improve understanding of the role of PVT1 in osteoarthritis, providing a novel possible target for osteoarthritis treatment.

Acknowledgements

Not applicable.

Funding

No funding was received.

Availability of data and materials

The datasets used during the present study are available from the corresponding author on reasonable request.

Authors' contributions

YM and SQ conceived and designed the experiments and performed the experiments. LS wrote the paper and performed the experiments. JZ conceived and designed the experiments and reviewed drafts of the paper. All authors read and approved the final manuscript.

Ethics approval and consent to participate

The present study was authorized by the Ethics Committee of Weihai Municipal Hospital. All patients with osteoarthritis and the healthy subjects who participated in the present study signed written informed consent.

Patient consent for publication

Not applicable.

Competing interests

The authors declare that they have no competing interests.

References

1. Hussain SM, Neilly DW, Baliga S, Patil S and Meek R: Knee osteoarthritis: A review of management options. Scott Med J 61: 7-16, 2016.
2. Kurtz SM, Ong KL, Lau E, Widmer M, Maravic M, Gómez-Barrena E, de Pina Mde F, Manno V, Torre M, Walter WL, *et al*: International survey of primary and revision total knee replacement. Int Orthop 35: 1783-1789, 2011.
3. Zhen G, Wen C, Jia X, Li Y, Crane JL, Mears SC, Askin FB, Frassica FJ, Chang W, Yao J, *et al*: Inhibition of TGF-β signaling in mesenchymal stem cells of subchondral bone attenuates osteoarthritis. Nat Med 19: 704-712, 2013.
4. Taylor N: Nonsurgical management of osteoarthritis knee pain in the older adult. Clin Geriatr Med 33: 41-51, 2017.
5. Batista PJ and Chang HY: Long noncoding RNAs: Cellular address codes in development and disease. Cell 152: 1298-1307, 2013.
6. Schmitz SU, Grote P and Herrmann BG: Mechanisms of long noncoding RNA function in development and disease. Cell Mol Life Sci 73: 2491-2509, 2016.
7. Liu Q, Hu X, Zhang X, Dai L, Duan X, Zhou C and Ao Y: The TMSB4 pseudogene lncRNA functions as a competing endogenous RNA to promote cartilage degradation in human osteoarthritis. Mol Ther 24: 1726-1733, 2016.
8. Zhang Y, Wang F, Chen G, He R and Yang L: LncRNA MALAT1 promotes osteoarthritis by modulating miR-150-5p/AKT3 axis. Cell Biosci 9: 54, 2019.
9. Cao L, Wang Y, Wang Q and Huang J: LncRNA FOXD2-AS1 regulates chondrocyte proliferation in osteoarthritis by acting as a sponge of miR-206 to modulate CCND1 expression. Biomed Pharmacother 106: 1220-1226, 2018.
10. Cui M, You L, Ren X, Zhao W, Liao Q and Zhao Y: Long non-coding RNA PVT1 and cancer. Biochem Biophys Res Commun 471: 10-14, 2016.
11. Huang W, Lan X, Li X, Wang D, Sun Y, Wang Q, Gao H and Yu K: Long non-coding RNA PVT1 promote LPS-induced septic acute kidney injury by regulating TNFα and JNK/NF-κB pathways in HK-2 cells. Int Immunopharmacol 47: 134-140, 2017.
12. Feng F, Qi Y, Dong C and Yang C: PVT1 regulates inflammation and cardiac function via the MAPK/NF-κB pathway in a sepsis model. Exp Ther Med 16: 4471-4478, 2018.
13. Li Y, Li S, Luo Y, Liu Y and Yu N: LncRNA PVT1 regulates chondrocyte apoptosis in osteoarthritis by acting as a sponge for miR-488-3p. DNA Cell Biol 36: 571-580, 2017.
14. Bartel DP: MicroRNAs: Genomics, biogenesis, mechanism, and function. Cell 116: 281-297, 2004.
15. Krol J, Loedige I and Filipowicz W: The widespread regulation of microRNA biogenesis, function and decay. Nat Rev Genet 11: 597-610, 2010.
16. Wang X, Liao Z, Bai Z, He Y, Duan J and Wei L: MiR-93-5p promotes cell proliferation through down-regulating PPARGC1A in hepatocellular carcinoma cells by bioinformatics analysis and experimental verification. Genes (Basel) 9: 51, 2018.
17. Xiang Y, Liao XH, Yu CX, Yao A, Qin H, Li JP, Hu P, Li H, Guo W, Gu CJ and Zhang TC: MiR-93-5p inhibits the EMT of breast cancer cells via targeting MKL-1 and STAT3. Exp Cell Res 357: 135-144, 2017.
18. Zhang Y, Wei QS, Ding WB, Zhang LL, Wang HC, Zhu YJ, He W, Chai YN and Liu YW: Increased microRNA-93-5p inhibits osteogenic differentiation by targeting bone morphogenetic protein-2. PLoS One 12: e0182678, 2017.
19. Hua Q, Chen Y, Liu Y, Li M, Diao Q, Xue H, Zeng H, Huang L and Jiang Y: Circular RNA 0039411 is involved in neodymium oxide-induced inflammation and antiproliferation in a human bronchial epithelial cell line via sponging miR-93-5p. Toxicol Sci 170: 69-81, 2019.
20. Xue H, Tu Y, Ma T, Wen T, Yang T, Xue L, Cai M, Wang F and Guan M: miR-93-5p attenuates IL-1β-induced chondrocyte apoptosis and cartilage degradation in osteoarthritis partially by targeting TCF4. Bone 123: 129-136, 2019.
21. Harding CV, Heuser JE and Stahl PD: Exosomes: Looking back three decades and into the future. J Cell Biol 200: 367-371, 2013.
22. Valadi H, Ekström K, Bossios A, Sjöstrand M, Lee JJ and Lötvall JO: Exosome-mediated transfer of mRNAs and microRNAs is a novel mechanism of genetic exchange between cells. Nat Cell Biol 9: 654-659, 2007.
23. Lo Cicero A, Stahl PD and Raposo G: Extracellular vesicles shuffling intercellular messages: For good or for bad. Curr Opin Cell Biol 35: 69-77, 2015.
24. Buzas EI, György B, Nagy G, Falus A and Gay S: Emerging role of extracellular vesicles in inflammatory diseases. Nat Rev Rheumatol 10: 356-364, 2014.
25. Li ZL, Lv LL, Tang TT, Wang B, Feng Y, Zhou LT, Cao JY, Tang RN, Wu M, Liu H, *et al*: HIF-1α inducing exosomal microRNA-23a expression mediates the cross-talk between tubular epithelial cells and macrophages in tubulointerstitial inflammation. Kidney Int 95: 388-404, 2019.
26. Patel NA, Moss LD, Lee JY, Tajiri N, Acosta S, Hudson C, Parag S, Cooper DR, Borlongan CV and Bickford PC: Long noncoding RNA MALAT1 in exosomes drives regenerative function and modulates inflammation-linked networks following traumatic brain injury. J Neuroinflammation 15: 204, 2018.
27. Zhang HG, Liu C, Su K, Yu S, Zhang L, Zhang S, Wang J, Cao X, Grizzle W and Kimberly RP: A membrane form of TNF-alpha presented by exosomes delays T cell activation-induced cell death. J Immunol 176: 7385-7393, 2006.
28. Livak KJ and Schmittgen TD: Analysis of relative gene expression data using real-time quantitative PCR and the 2(-Delta Delta C(T)) method. Methods 25: 402-408, 2001.
29. Cao C, Yin C, Shou S, Wang J, Yu L, Li X and Chai Y: Ulinastatin protects against LPS-induced acute lung injury by attenuating TLR4/NF-κB pathway activation and reducing inflammatory mediators. Shock 50: 595-605, 2018.
30. Hare KB, Stefan Lohmander L, Kise NJ, Risberg MA and Roos EM: Middle-aged patients with an MRI-verified medial meniscal tear report symptoms commonly associated with knee osteoarthritis. Acta Orthop 88: 664-669, 2017.
31. Huang ZY, Stabler T, Pei FX and Kraus VB: Both systemic and local lipopolysaccharide (LPS) burden are associated with knee OA severity and inflammation. Osteoarthritis Cartilage 24: 1769-1775, 2016.

32. Zhao C, Wang Y, Jin H and Yu T: Knockdown of microRNA-203 alleviates LPS-induced injury by targeting MCL-1 in C28/I2 chondrocytes. Exp Cell Res 359: 171-178, 2017.
33. Sun T, Yu J, Han L, Tian S, Xu B, Gong X, Zhao Q and Wang Y: Knockdown of long non-coding RNA RP11-445H22.4 alleviates LPS-induced injuries by regulation of miR-301a in osteoarthritis. Cell Physiol Biochem 45: 832-843, 2018.
34. Li F, Sun J, Huang S, Su G and Pi G: LncRNA GAS5 overexpression reverses LPS-induced inflammatory injury and apoptosis through up-regulating KLF2 expression in ATDC5 chondrocytes. Cell Physiol Biochem 45: 1241-1251, 2018.
35. Chen WK, Yu XH, Yang W, Wang C, He WS, Yan YG, Zhang J and Wang WJ: lncRNAs: Novel players in intervertebral disc degeneration and osteoarthritis. Cell Prolif 50: e12313, 2017.
36. Xu J and Xu Y: The lncRNA MEG3 downregulation leads to osteoarthritis progression via miR-16/SMAD7 axis. Cell Biosci 7: 69, 2017.
37. Barile L and Vassalli G: Exosomes: Therapy delivery tools and biomarkers of diseases. Pharmacol Ther 174: 63-78, 2017.
38. Zhao Y, Zhao J, Guo X, She J and Liu Y: Long non-coding RNA PVT1, a molecular sponge for miR-149, contributes aberrant metabolic dysfunction and inflammation in IL-1β-simulated osteoarthritic chondrocytes. Biosci Rep 38: BSR20180576, 2018.
39. Ding LB, Li Y, Liu GY, Li TH, Li F, Guan J and Wang HJ: Long non-coding RNA PVT1, a molecular sponge of miR-26b, is involved in the progression of hyperglycemia-induced collagen degradation in human chondrocytes by targeting CTGF/TGF-β signal ways. Innate Immun 26: 204-214, 2020.
40. Liu J, Jiang M, Deng S, Lu J, Huang H, Zhang Y, Gong P, Shen X, Ruan H, Jin M and Wang H: miR-93-5p-containing exosomes treatment attenuates acute myocardial infarction-induced myocardial damage. Mol Ther Nucleic Acids 11: 103-115, 2018.
41. Laursen TL, Støy S, Deleuran B, Vilstrup H, Grønbaek H and Sandahl TD: The damage-associated molecular pattern HMGB1 is elevated in human alcoholic hepatitis, but does not seem to be a primary driver of inflammation. APMIS 124: 741-747, 2016.
42. Srikrishna G and Freeze HH: Endogenous damage-associated molecular pattern molecules at the crossroads of inflammation and cancer. Neoplasia 11: 615-628, 2009.
43. Qin Y, Chen Y, Wang W, Wang Z, Tang G, Zhang P, He Z, Liu Y, Dai SM and Shen Q: HMGB1-LPS complex promotes transformation of osteoarthritis synovial fibroblasts to a rheumatoid arthritis synovial fibroblast-like phenotype. Cell Death Dis 5: e1077, 2014.
44. Wang X, Guo Y, Wang C, Yu H, Yu X and Yu H: MicroRNA-142-3p inhibits chondrocyte apoptosis and inflammation in osteoarthritis by targeting HMGB1. Inflammation 39: 1718-1728, 2016.
45. Liang S, Lv ZT, Zhang JM, Wang YT, Dong YH, Wang ZG, Chen K, Cheng P, Yang Q, Guo FJ, *et al*: Necrostatin-1 attenuates trauma-induced mouse osteoarthritis and IL-1β induced apoptosis via HMGB1/TLR4/SDF-1 in primary mouse chondrocytes. Front Pharmacol 9: 1378, 2018.
46. Jiang Y, Zhu L, Zhang T, Lu H, Wang C, Xue B, Xu X, Liu Y, Cai Z, Sang W, *et al*: BRD4 has dual effects on the HMGB1 and NF-κB signalling pathways and is a potential therapeutic target for osteoarthritis. Biochim Biophys Acta Mol Basis Dis 1863: 3001-3015, 2017.